

Computing the flow past a cylinder with free hemispherical ends

G. J. Sheard* M. C. Thompson K. Hourigan

13 September 2004

Abstract

A novel application of a spectral-element method with a Fourier expansion in the third dimension is used to compute the flow past a cylinder with free hemispherical ends. A cylinder with free hemispherical ends has the useful property of being a sphere at the small-length-ratio limit, while approaching a straight circular cylinder as the length ratio increases. 128 Fourier planes were required to resolve the flow to better than 1% accuracy in Strouhal frequency and mean drag measurements. A coarser grid with 64 planes provided measured forces within approximately 2% accuracy, but Strouhal frequencies were over-predicted by approximately 8%.

The measured Strouhal frequencies will prove useful as benchmark data for future low-Reynolds-number studies of the flow past short cylinders.

Contents

1	Introduction	2
2	Numerical methodology	2
2.1	Geometry-specific treatment	3
2.2	Comparison of methods for the flow past a sphere	4
3	An axial force oscillation at small length ratios	4

*Fluids Laboratory for Aeronautical and Industrial Research (FLAIR), Dept. of Mechanical Engineering, Monash University, Melbourne, AUSTRALIA. Greg.Sheard@eng.monash.edu.au

4	Wake symmetry and shedding frequencies at larger length ratios	6
5	Concluding remarks and direction for further study	8

1 Introduction

An efficient alternative to the application of three-dimensional meshes to model the flow past bodies that contain geometric symmetries [1, 12] is to utilise the symmetry properties of the body to simplify the mesh formulation. Examples of this include the numerous numerical studies that have used the span-wise uniformity of a straight circular cylinder [6, 3, 2] or the azimuthal symmetry of a sphere [20, 19, 18] to model the flow using a two-dimensional plane grid, and modeling the variation in flow variables in the third dimension using a Fourier expansion.

This same technique was employed to good result in the determination of the stability properties of the flow past rings [14, 15, 16]. The ring is an example of a body that can vary smoothly from a sphere towards a straight circular cylinder as a geometric parameter is varied. A circular cylinder with free hemispherical ends is another such body, and has been the subject of recent experimental studies [13, 11] aimed at exploiting this property in reference to the study of circular cylinders with small aspect ratios [8, 7]. It is convenient to define a coordinate system relative to the cylinder as shown in Figure 1.

The Reynolds number ($Re = Ud/\nu$) range of interest in this study is $Re \lesssim 300$, where U is the free-stream velocity, d is the cross-section diameter of the cylinder, and ν is the kinematic viscosity of the fluid. This range encompasses the transitions to unsteady and three-dimensional flows in the wakes behind spheres and circular cylinders.

A cylinder with free hemispherical ends differs from the aforementioned bodies in that the symmetry axis of the body is normal to the direction of flow rather than parallel. The details of the numerical treatment of this body is discussed in the section to follow.

2 Numerical methodology

This study employs the same spectral-element code that has been used previously to compute the three-dimensional flow past circular cylinders [17], spheres [18] and rings [16].

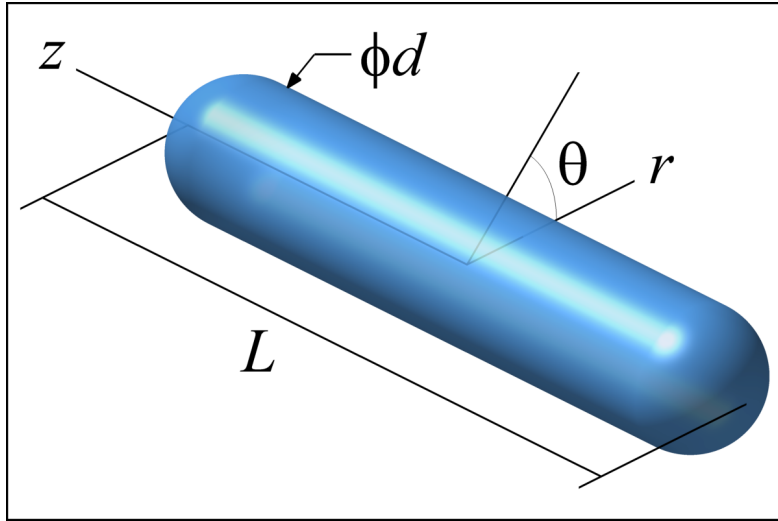


Figure 1: The coordinate system relative to a cylinder with free hemispherical ends. The direction of flow is across a plane of constant z , and the length ratio $L_R = L/d$.

For details regarding the spatial discretisation and temporal integration employed as part of the numerical scheme, see [9, 20, 5]. In brief, the computational domain in an r - z plane of symmetry was discretised as a grid of elements. The elements were concentrated in regions where high spatial gradients in the velocity and pressure were anticipated (i.e., downstream and in the vicinity of the cylinder). The pressure and velocity fields were represented by a Fourier expansion in the θ direction. Within each element, high-order Lagrangian tensor-product polynomial basis functions were employed, and integration over the computational domain was based on a Galerkin finite-element method.

Temporal integration of the incompressible Navier–Stokes equations was carried out using a three-step operator splitting scheme, whereby the non-linear advection, pressure and diffusion steps were each treated separately. The advection term was integrated using an explicit 3rd-order Adams–Bashforth scheme, the pressure term was set up to satisfy conservation of mass and was solved as a Poisson equation, and the diffusion term was solved using an implicit 2nd-order Crank–Nicholson scheme.

2.1 Geometry-specific treatment

In order to resolve the flow normal to a cylinder, a high number of Fourier planes are required. This imposes a restriction on the time-step due to the

Courant condition, as the spatial wavelength of the Fourier modes are proportional to r , and hence approach zero as $r \rightarrow 0$. This imposes a severe time-step restriction due to the Courant condition. A filter was applied to the higher Fourier modes at small radial distances from the symmetry axis to mitigate this restriction.

To maximise the computational efficiency of the study, the first task was to determine the optimum number of elements and Fourier planes for the computations. Tests were performed on a sphere modeled using the present “crossflow” flow direction, and these were compared to numerical studies of a sphere that employed a traditional axial-flow method [18, 16].

2.2 Comparison of methods for the flow past a sphere

The element distribution over the r - z plane followed closely to past numerical studies for similar Reynolds number ranges (e.g., [2, 16]). Elements were concentrated close to the cylinder surface to resolve the boundary-layer, and over the domain downstream of the cylinder to capture the axial variation in the wake.

Figure 2 shows the convergence of global flow quantities with an increase in the element order N^2 . The results are compared to a highly resolved computation with flow in an axial direction from [16]. A convergence to within 1% for the pressure and viscous components of mean drag (C_{D_p} and C_{D_v} , respectively) and the Strouhal frequency (St) is desired for this study, and this was only achieved by employing a mesh with 128 planes. The radial dispersal of grid lines away from the cylinder means that resolution drops very rapidly with increasing r . This loss of resolution is apparent from the plots in Figure 3, in which (a) and (b) show the wakes computed using the crossflow grids, and (c) shows an accurate axial-flow computation. The under-resolved nature of the 64-plane computation is especially evident in Figure 3(a).

The meshes employed in this study typically comprise 100 macro-elements (plus additional elements along the varying straight-span section), each containing $11^2 = 121$ interpolation points.

3 An axial force oscillation at small length ratios

For cylinders with length ratios $1 \leq L_R \leq 4$, an axial oscillation in the force imparted on the cylinder was detected. A plot of the variation in the Strouhal frequency of this oscillation with length ratio is given in Figure 4. The spherical nature of a cylinder with $L_R = 1$ means that there is no specific

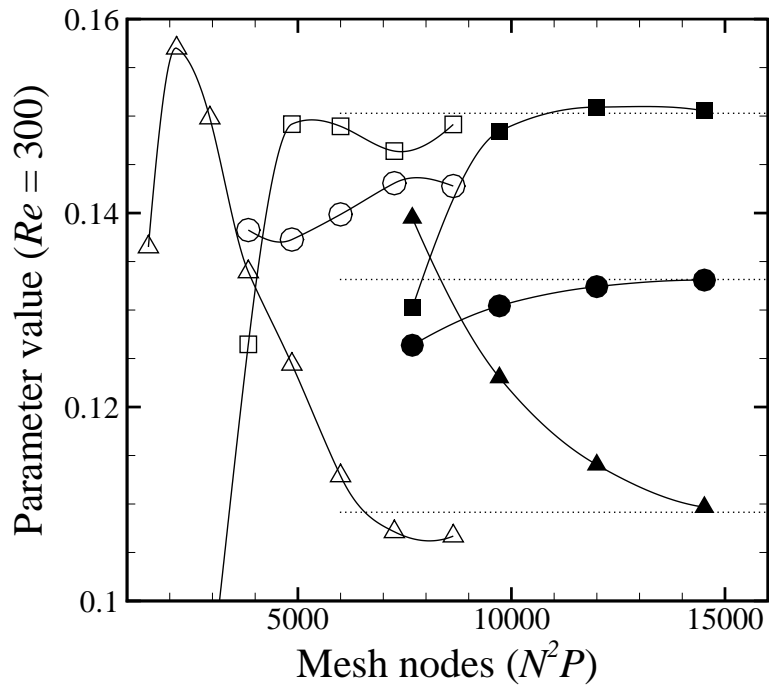


Figure 2: Convergence of global flow quantities for a sphere ($L_R = 1$) at $Re = 300$ with increasing resolution (N^2P). Meshes with $P = 64$ and 128 planes (open and filled symbols, respectively) are shown, and quantities C_{D_p} (\square), C_{D_v} (\triangle) and St (\circ) are monitored. The dotted lines show accurate measurements from an axial-flow computation.

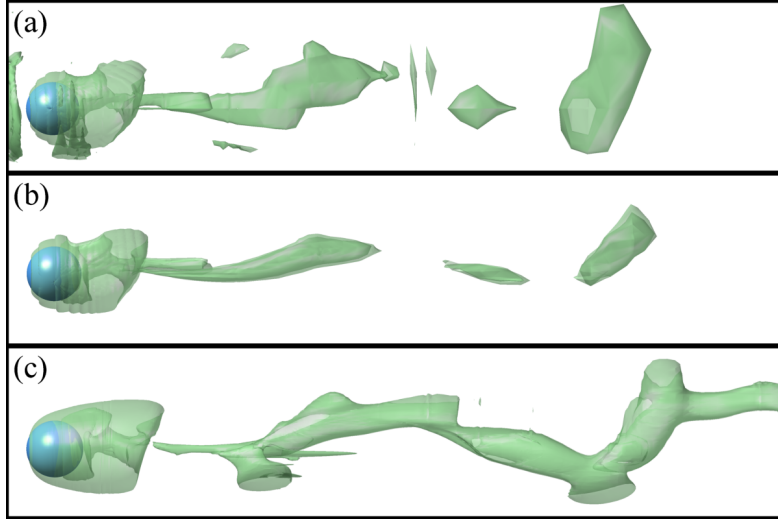


Figure 3: A comparison between the crossflow computations with 64 (a) and 128 (b) planes and an accurate axial-flow computation. Flow is from left to right, and the translucent isosurface shows the vortical structure of the wake.

orientation in which unsteady flow may develop. The Strouhal frequency for a sphere is included in the plot as it appears to be a natural extrapolation of the $St-L_R$ trend to $L_R = 1$. This implies that the plane in which vorticity is shed from a sphere in the well-known hairpin wake [4, 19] is orthogonal to the plane in which the Kármán wake forms behind a circular cylinder. It is therefore expected that for cylinders with intermediate length ratios ($1 < L_R \ll \infty$), it should be possible to detect the both of these instabilities in the wake. No evidence of such a measurement has yet been reported in the literature.

4 Wake symmetry and shedding frequencies at larger length ratios

Computed mean drag and Strouhal frequency measurements were obtained for a sphere over a range of Reynolds numbers up to $Re = 300$. These results were in agreement to within 1% of previously reported values. The present study tested cylinders with length ratios $1 \leq L_R \leq 10$, and results indicate that although the critical Reynolds number for the onset of vortex shedding for this cylinder is within 10-20% of the corresponding value for a straight circular cylinder ($Re_c \approx 47$ [10]), there is a large discrepancy in the Strouhal-Reynolds number profiles shown in Figure 5. These measurements show that

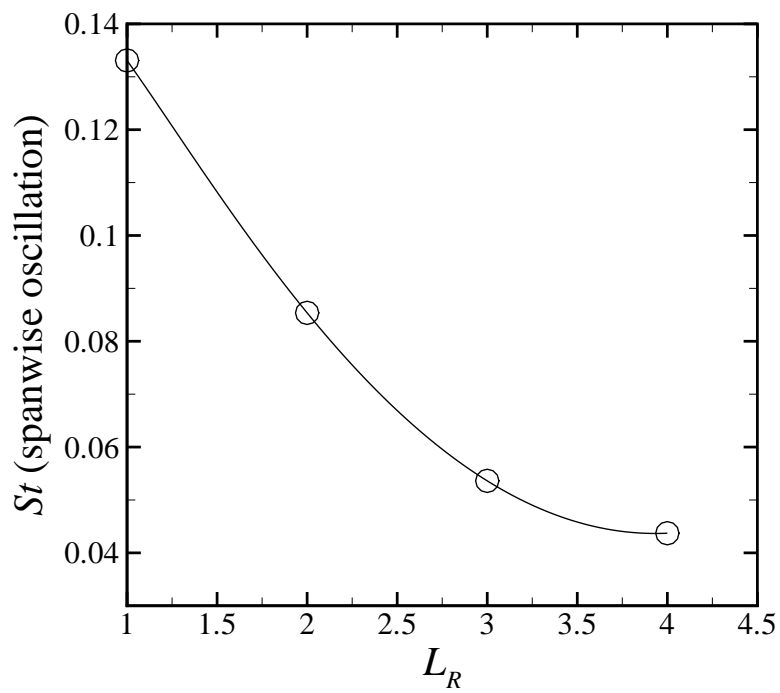


Figure 4: A plot of the Strouhal frequency against length ratio for the periodic axial body-force oscillation at $Re = 300$.

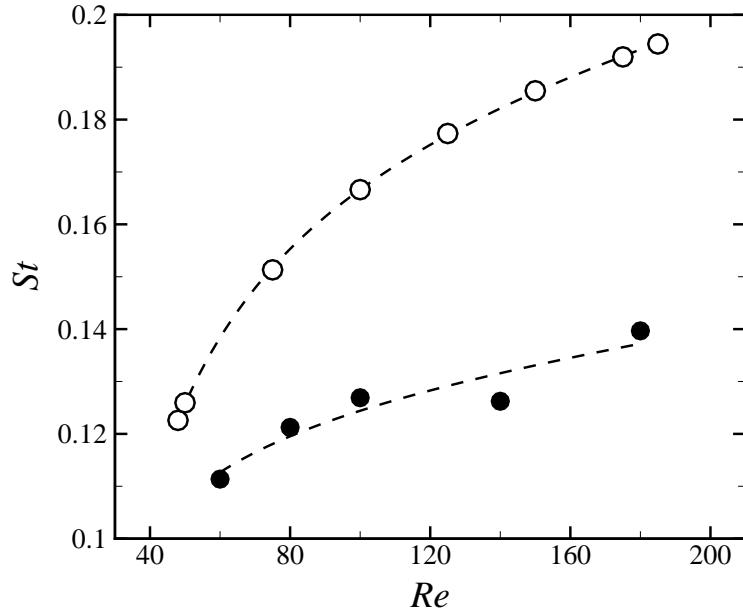


Figure 5: Strouhal–Reynolds number profiles for a cylinder with $L_R = 10$ (solid circles), and a straight circular cylinder (open circles). Dashed guidance lines show a least-squares fit to a function of the form $St = ARe + B + C/Re$.

the three-dimensional effects created by the flow over the free hemispherical ends has a significant influence on the shedding characteristics of the wake. It should be noted that a zero axial force was measured for all Reynolds numbers with $L_R = 10$, whereas cylinders with $1 \leq L_R \leq 5$ all exhibited non-zero axial forcing. A wake symmetry about the cylinder half-span is therefore broken at some length ratio in the range $5 < L_R < 10$.

5 Concluding remarks and direction for further study

At smaller length ratios ($L_R = L/d \lesssim 5$), the cylinder experiences forcing in both a transverse and an axial direction, suggesting that the flow is not symmetrical about the cylinder mid-point. The flow is symmetrical about the cylinder half-span for cylinders with $L_R \gtrsim 10$.

Further computations are being carried out to determine the non-linear properties of the first-occurring Hopf bifurcations in the wakes of short- and long-length-ratio cylinders.

Acknowledgements: The computing resources of both the Australian Partnership for Advanced Computing (APAC) National Facility and the Victorian Partnership for Advanced Computing (VPAC) were employed for this study. This research was supported by an ARC Linkage International grant.

References

- [1] A. Brydon and M. C. Thompson. Flow interaction between two spheres at moderate Reynolds number. In B. B. Dally, editor, *Proceedings of the Fourteenth Australasian Fluid Mechanics Conference*, pages 693–696, Department of Mechanical Engineering, Adelaide University, S.A. 5005, Australia, 2001. Published by Adelaide University.
- [2] R. D. Henderson. Non-linear dynamics and pattern formation in turbulent wake transition. *J. Fluid Mech.*, 352:65–112, 1997.
- [3] R. D. Henderson and D. Barkley. Secondary instability in the wake of a circular cylinder. *Phys. Fluids*, 8:1683–1685, 1996.
- [4] T. A. Johnson and V. C. Patel. Flow past a sphere up to a Reynolds number of 300. *J. Fluid Mech.*, 378:19–70, 1999.
- [5] G. E. Karniadakis and S. J. Sherwin. *Spectral/hp Element Methods for CFD*. Oxford University Press, 1999.
- [6] G. E. Karniadakis and G. S. Triantafyllou. Three-dimensional dynamics and transition to turbulence in the wake of bluff objects. *J. Fluid Mech.*, 238:1–30, 1992.
- [7] N. W. M. Ko, C. W. Law, and K. W. Lo. Mutual interference on transition of wake of circular cylinder. *Phys. Fluids*, 12:1–34, 1962.
- [8] C. Norberg. An experimental investigation of the flow around a circular cylinder: Influence of aspect ratio. *J. Fluid Mech.*, 258:287–316, 1994.
- [9] A. T. Patera. A spectral element method for fluid dynamics: Laminar flow in a channel expansion. *J. Comp. Phys.*, 54:468–488, 1984.
- [10] M. Provansal, C. Mathis, and L. Boyer. Bénard-von Kármán instability: Transient and forced regimes. *J. Fluid Mech.*, 182:1–22, 1987.
- [11] M. Provansal, L. Schouveiler, and T. Leweke. From the double vortex street behind a cylinder to the wake of a sphere. *Euro. J. Mech. B (Fluids)*, 23:65–80, 2004.

- [12] L. Schouveiler, A. Brydon, T. Leweke, and M. C. Thompson. Interactions of the wakes of two spheres placed side by side. *J. Fluids Struct.*, 23:137–145, 2004.
- [13] L. Schouveiler and M. Provansal. Periodic wakes of low aspect ratio cylinders with free hemispherical ends. *J. Fluids Struct.*, 14:565–573, 2001.
- [14] G. J. Sheard, M. C. Thompson, and K. Hourigan. From spheres to circular cylinders: The stability and flow structures of bluff ring wakes. *J. Fluid Mech.*, 492:147–180, 2003.
- [15] G. J. Sheard, M. C. Thompson, and K. Hourigan. Asymmetric structure and non-linear transition behaviour of the wakes of toroidal bodies. *Euro. J. Mech. B (Fluids)*, 23(1):167–179, 2004.
- [16] G. J. Sheard, M. C. Thompson, and K. Hourigan. From spheres to circular cylinders: Non-axisymmetric transitions in the flow past rings. *J. Fluid Mech.*, 506:45–78, 2004.
- [17] M. C. Thompson, K. Hourigan, and J. Sheridan. Three-dimensional instabilities in the wake of a circular cylinder. *Exp. Therm. Fluid Sci.*, 12:190–196, 1996.
- [18] M. C. Thompson, T. Leweke, and M. Provansal. Kinematics and dynamics of sphere wake transition. *J. Fluids Struct.*, 15:575–585, 2001.
- [19] A. G. Tomboulides and S. A. Orszag. Numerical investigation of transitional and weak turbulent flow past a sphere. *J. Fluid Mech.*, 416:45–73, 2000.
- [20] A. G. Tomboulides, S. A. Orszag, and G. E. Karniadakis. Direct and large-eddy simulation of the flow past a sphere. In *Proceedings of the Second International Conference on Turbulence Modeling and Experiments (2nd ICTME)*, Florence, Italy, 1993.